Advection of a Passive Scalar over a Finite-Amplitude Ridge in a Stratified Rotating Atmosphere

WILLIAM BLUMEN AND BRIAN D. GROSS

Department of Astrophysical, Planetary and Atmospheric Sciences, University of Colorado, Boulder, CO 80309

(Manuscript received 30 July 1986, in final form 14 December 1986)

ABSTRACT

A basic uniform current flows over a two-dimensional finite-amplitude ridge of characteristic scale L and amplitude ϵ. The disturbance field is constrained by the geostrophic momentum approximation, by uniform potential vorticity (uniform Brunt–Väisälä frequency N) and by the constant Coriolis parameter f. Solutions are represented as the sum of a steady disturbance, recently found by Blumen and Gross, and a relatively weak translating disturbance. The translating disturbance is a passive scalar that is advected by the steady mountain circulation. The propagation speed over a ridge in an unbounded atmosphere is shown to increase with the parameter ϵ/D, where $D = fL/N$ is the deformation depth. The steady mountain circulation produces frontolysis in the disturbance field on the windward slope and frontogenesis on the leeward slope. These frontogenetical features are primarily controlled by the steady horizontal velocity, which is divergent on the windward side and convergent in the lee. The steady mountain circulation also disrupts the initial state of thermal wind balance imposed on the disturbance potential temperature and cross-stream velocity fields. An approximate evaluation of the ageostrophic circulation required to restore thermal wind balance is provided. This circulation, which may be direct or indirect, is related to the spatial structure of the initial disturbance and to its relative position on the ridge. Comparison with a related study by Bannon, and an evaluation of the principal limitations of both models complete the study.

1. Introduction

Considerable efforts have been directed to finding solutions for *steady,* stratified rotating flow over orography. Analytic solutions may sometimes be found (e.g., Robinson, 1960), more frequently numerical methods are required (e.g., Merkine and Kálnay-Rivas, 1976), and it is not unusual to combine both approaches (e.g., Bannon, 1986). *Time-dependent* solutions are not easily obtained, and invariably numerical simulations must be used (e.g., Pierrehumbert and Wyman, 1985). There have, however, been exceptions. These include the combined numerical and analytical study of transient flow by Huppert and Bryan (1976), and the analytical time-dependent quasi-geostrophic and semigeostrophic model studies of Bannon (1983, 1984).

The present investigation falls into the latter class of models. It has been motivated by the availability of a relatively detailed set of observations obtained during the field phase of ALPEX. The observing system, in place during March and April 1982, included microbarograph arrays, increased radiosonde coverage, radar and instrumented aircraft probes. This database appears to be relatively sound for analyses of frontal interaction with orography, particularly data obtained during Intensive Observing Periods (IOPs). Data analyses are currently being carried out at many institutions and results should begin to accumulate in the near future.

However, there are relatively few theoretical studies of frontal interaction with orography that may be used in conjunction with observational analyses. Bannon's work, just cited, and Davies (1984) stand out, but there are apparently few others. The present study of a prototype model is designed to extract some fundamental properties that characterize the translation of a disturbance over a ridge. In many respects the model is similar to the one presented by Bannon (1984). The model is two-dimensional and inviscid; semi-geostrophic dynamics and uniform potential vorticity flow are considered. However, there are some important differences: 1) A *finite-amplitude* ridge is employed, and the lower boundary condition is satisfied exactly by the basic flow and the translating disturbance. 2) There is a steady ageostrophic circulation associated with the basic flow, but there is no ageostrophic circulation associated with the disturbance: the steady flow controls the behavior of the cross-stream velocity and temperature fields, which are treated as passive scalars. Despite the simplicity of this model it does provide relatively clear-cut predictions that may be compared to observed features, when detailed analyses become available and to features predicted by more complex models of a front or a disturbance moving over orography. The following features are presented: a) the translation speed of the dis-

turbance as a function of the ridge height; b) the contributions to frontogenesis–frontolysis from the steady ageostrophic divergence field and from the tilting effect of upslope (downslope) translation; c) an estimate of the forced ageostrophic circulation that would be required to restore the thermal wind balance, disrupted by the steady mountain circulation. This latter feature is provided as a relatively weak secondary effect, since the steady mountain circulation is assumed to control the displacement of the disturbance field.

The model is developed in section 2. The solution, displaying the temporal and spatial dependence of a passive scalar advected by a steady flow, is derived in section 3. The translation speed is presented in section 4, and the frontogenetical–frontolytical properties of the disturbance appear in section 5. Features of the forced circulation, required to restore thermal wind balance, are considered in section 6, while a comparison with Bannon's model and some final remarks are contained in section 7.

2. Model

A steady current and a translating disturbance are forced over a finite-amplitude ridge. The flow is inviscid and adiabatic, and contained within a channel of depth H. The basic system of equations employs the geostrophic momentum approximation, and the potential vorticity is assumed to be constant. These equations, presented by Hoskins (1975), are

$$\partial v_g/\partial t + (u_g + u_a)\partial v_g/\partial x + w\partial v_g/\partial z = -fu_a, \quad (1)$$

$$\partial u_a/\partial x + \partial w/\partial z = 0, \quad (2)$$

$$\partial\theta/\partial t + (u_g + u_a)\partial\theta/\partial x + w(N^2 + \partial\theta/\partial z) = 0, \quad (3)$$

where x is directed downstream, z is the vertical coordinate and t time. The steady geostrophic current is uniform, i.e., u_g = constant. The cross-stream geostrophic velocity v_g is in thermal wind balance:

$$\partial\theta/\partial x = f\partial v_g/\partial z. \quad (4)$$

The ageostrophic velocity component is u_a and w is the vertical velocity. The potential temperature field is separated into a basic part, depending only on z, and a disturbance θ^*, represented by $\theta = g\theta^*/\theta_0$ in (3) and (4); θ_0 is a constant standard value and g is the acceleration of gravity. The constant Brunt–Väisälä frequency, associated with the basic potential temperature field, is denoted by N, and the constant Coriolis parameter is f.

The field of velocity and potential temperature may be separated into steady and time-dependent components as

$$\left.\begin{aligned} u &= u_g + \bar{u}_a(x,z) + u'_a(x,z,t) \\ v &= \bar{v}_g(x,z) + \bar{v}_a(x,z) + v'_g(x,z,t) \\ w &= \bar{w}(x,z) + w'(x,z,t) \\ \theta &= \bar{\theta}(x,z) + \theta'(x,z,t) \end{aligned}\right\}. \quad (5)$$

The kinematic condition at the lower boundary is

$$\bar{w} + w' = (u_g + \bar{u}_a + u'_a)\partial\epsilon h(x)/\partial x, \quad z = \epsilon h(x) \quad (6)$$

where ϵ represents the amplitude and $h(x)$ the shape of the lower boundary. At the upper lid, the appropriate condition is

$$\bar{w} = w' = 0, \quad z = H \quad (7)$$

and all variables vanish as $H \to \infty$. The lateral boundary conditions will be considered later.

Separation of the steady and time-dependent expressions in (6) yields

$$\bar{w} = (u_g + \bar{u}_a)\partial\epsilon h(x)/\partial x, \quad (8a)$$

$$w' = u'_a\partial\epsilon h(x)/\partial x. \quad (8b)$$

Both (8a, b) are evaluated on the boundary $z = \epsilon h(x)$. The boundary conditions for the time-dependent disturbances, (7) and (8b), only contain ageostrophic velocity components (u'_a, w'). These boundary conditions may be satisfied by setting

$$u'_a = w' = 0 \quad (9)$$

both on the boundaries *and* in the interior flow. The nontrivial time-dependent solutions that result from this constraint (9) will be determined in section 3.

The equations (1)–(4) are satisfied separately by the steady and by the time-dependent terms, defined in (5). Some steady-state solutions have been presented by Blumen and Gross (1986; hereafter referred to as BG). The solution corresponding to a uniform basic flow will be used to solve the time-dependent system, which reduces to (9) and

$$\partial v'/\partial t + (u_g + \bar{u}_a)\partial v'/\partial x + \bar{w}\partial v'/\partial z = 0, \quad (10)$$

$$\partial\theta'/\partial t + (u_g + \bar{u}_a)\partial\theta'/\partial x + \bar{w}\partial\theta'/\partial z = 0. \quad (11)$$

Since a time-dependent ageostrophic circulation is not maintained, as a consequence of (9), the thermal wind balance (4) need not be satisfied by θ' and v'_g; this point is established by omission of the "geostrophic" subscript g in (10). The advecting velocities ($\bar{u}_a$, $\bar{w}$) are assumed to be known solutions of the steady-state equations that satisfy the nonlinear boundary condition (8a) and the upper boundary condition (7). For this case of uniform basic flow, the cross-stream ageostrophic velocity is $\bar{v}_a = 0$.

All terms are put into nondimensional form, as in BG, and geostrophic coordinates are introduced as

$$\bar{X} = x + \mathrm{Ro}\bar{v}_g(x,z), \quad Z = z, \quad T = t, \quad (12)$$

where $\mathrm{Ro} \leqslant 0.3$ is the Rossby number based on the velocity scale u_g and the characteristic width of the ridge L. The notation $\bar{X}$, in (12) indicates that the time-dependent velocity $v'(x, z, t)$ has been *omitted* in the definition of the geostrophic coordinate. Introduction of (12) into (10) and (11) and use of Hoskin's (1975) transformation formulas provides the nondimensional equations:

$$\partial v'/\partial T + \partial v'/\partial \bar{X} + \bar{w}\partial v'/\partial Z = 0, \quad (13)$$

$$\partial \theta'/\partial T + \partial \theta'/\partial \bar{X} + \bar{w}\partial \theta'/\partial Z = 0. \quad (14)$$

The Rossby number Ro does not appear in either (13) or (14), since it may be absorbed into the definition of each variable. In this form, v' and θ' are passive scalars advected by a uniform wind $u_g = 1$, and by a steady vertical velocity field $\bar{w}(\bar{X}, Z)$ produced by flow over a ridge. The ageostrophic velocity component $\bar{u}_a$ is absorbed into the coordinate transformation, and its effect on the distribution of v' and θ' is not apparent until the physical space representation is recovered.

3. Solutions

a. Isentropic coordinates

Both the top and bottom boundaries are isentropic surfaces satisfying

$$\Theta = Z + \bar{\theta}(\bar{X}, Z), \quad (15)$$

where Θ is the total time-independent potential temperature field. Adiabatic flow,

$$d\Theta/dT = \partial\bar{\theta}/\partial\bar{X} + \bar{w}(1 + \partial\bar{\theta}/\partial Z) = 0, \quad (16)$$

is assumed by BG, so that transformation to Θ coordinates is appropriate. Introduction of the usual transformation relationships (e.g., Kasahara, 1974) into (13) and (14), and use of (16), yields

$$(\partial/\partial T + \partial/\partial\bar{X})g = 0, \quad (17)$$

where $g = g(\bar{X}, \Theta, T)$ and differentiation is along surfaces Θ = constant. Specifically, g represents either v' or θ'. Solutions are given by

$$g = g(\bar{X} - \bar{T}, \Theta). \quad (18)$$

This solution (18) will be used to examine the effect on the translation speed (in physical space) and the frontogenetical/frontolytical features imposed on the disturbance by the steady mountain circulation.

According to (18), both v' and θ' will conserve their initial values on Θ surfaces. Far upstream, where isentropic surfaces are level, the initial disturbance field is required to satisfy both thermal wind balance

$$\partial\theta'/\partial\bar{X} - \partial v'/\partial Z = 0 \quad (19)$$

and the uniform potential vorticity requirement

$$\partial v'/\partial\bar{X} + \partial\theta'/\partial Z = 0. \quad (20)$$

The solutions for v' and θ' may be used to display the imbalances that develop when the disturbances move over the ridge. A time dependent ageostrophic circulation would be required to maintain the balances, (19) and (20), against possible imbalances imposed by the mountain circulation. Consequently, this prototype model can provide a relatively simple and straightforward assessment of the time-dependent circulation needed to maintain a balanced state.

b. Steady solutions

Steady solutions represented by uniform upstream flow over a finite-amplitude ridge in a channel of depth H were obtained by BG. These solutions are used to represent the quantities $\bar{u}_a$, $\bar{w}$, $\bar{v}_g$ and Θ that appear in the advection equation (10), in the coordinate transformation (12) and in the representation of the isentropic surfaces (15). The ageostrophic velocity field $\bar{u}_a$ is displayed in BG (Fig. 4), the streamfield in BG (Fig. 7b), the cross-stream geostrophic velocity $\bar{v}_g$ in BG (Fig. 5) and Θ is represented by BG [eq. (43b)]. The lower boundary, appearing in BG, as well as in this study is represented as Θ = constant in the various figures presented. The field of Θ surfaces is symmetric above the lower boundary, and the amplitude decays to zero at the level upper lid.

c. Time-dependent solutions

Solutions of the form represented by (18) are provided by

$$\theta' = \alpha \ln\left\{\frac{\sinh^2[\pi D(\bar{\chi}+\beta)/2H] + \sin^2(\pi D\Theta/2H)}{\sinh^2[\pi D(\bar{\chi}-\beta)/2H] + \sin^2(\pi D\Theta/2H)}\right\} + \text{constant}, \quad (21)$$

$$v' = -\alpha \tan^{-1}\left\{\frac{\sinh 2(\pi D\beta/2H)\sin 2(\pi D\Theta/2H)}{\cosh 2(\pi D\bar{\chi}/2H) - \cosh 2(\pi D\beta/2H)\cos 2(\pi D\Theta/2H)}\right\} + \text{constant}, \quad (22)$$

where $\bar{\chi} = \bar{X} - \bar{X}_0 - T$, $\bar{X}_0 = 8$ and $\Theta \to Z = z$ upstream. The added constant in (21) is used to adjust the initial position of the zero contour; then the added constant in (22) is determined by the requirement that one of the zero contours of the symmetric disturbance v' coincide with $\theta' = 0$ at ground level. The quantities (α, β) determine the strengths of the field in (21) and (22). The distributions of (θ', v') are shown at time $T = 3$ in Fig. 1. These solutions, which are similar to those used by BG [Eqs. (43a, b)], do satisfy both thermal wind balance (19) and the constraint of uniform potential vorticity (20) *upstream* at $T = 0$.

The gradients of θ' and v', shown in Fig. 1, are approximately 0.6 K/100 km and 1 m s^{-1}/100 km, respectively, based on typical scales associated with Ro ≈ 0.3. The translations of these fields over the ridge are shown in Figs. 2 and 3. These figures reveal that both the translation speed and the gradients of the disturbance field vary with distance over the slopes. Yet no net change occurs; the disturbances recover their initial values on the level surface downstream. A reversal of the disturbance fields in (21) and (22), to provide a cyclonic shear and a symmetric potential tem-

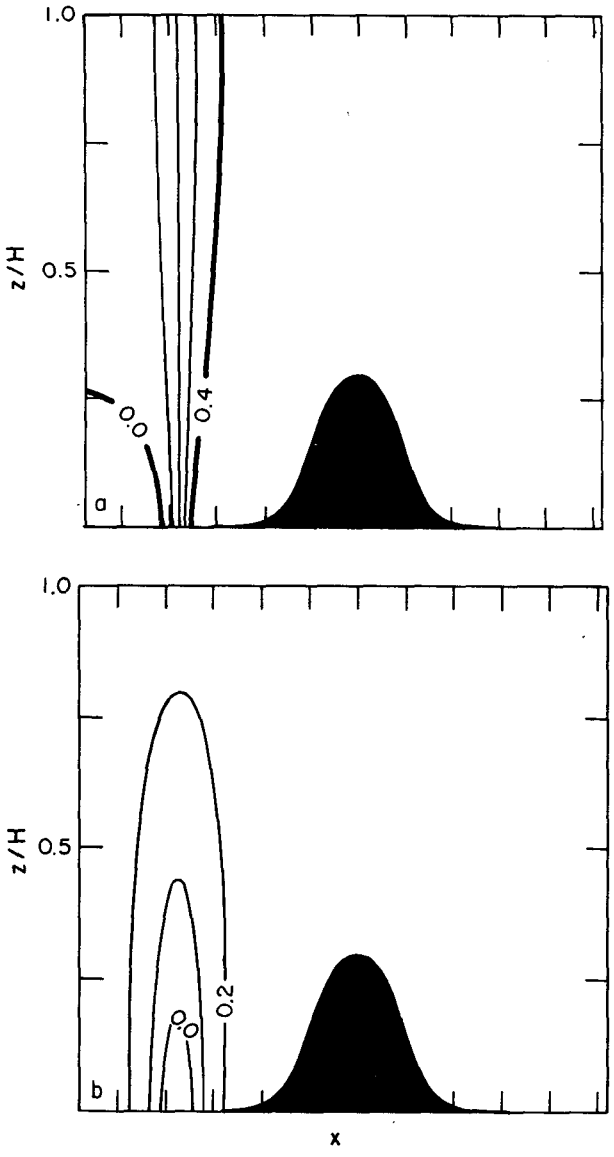

FIG. 1. (a) Disturbance potential temperature field θ', expressed by (21), at time $T = 3$. The x-axis is scaled in units of the half-width of the ridge. The crest is at $z = 0.3H$, where H denotes the depth of the atmosphere. The contour interval is 0.1, and the surface gradient corresponds to 0.6 K/100 km. (b) Disturbance cross-stream velocity v', expressed by (22), at time $T = 3$. The contour interval is 0.1, and the maximum surface gradients correspond to 1 m s^{-1}/100 km.

perature disturbance, only requires a reinterpretation of the present results.

4. Translation speed

The translation speed of disturbances expressed by (18) is uniform in geostrophic–isentropic coordinate space. However, in the transformation to physical space both $\bar{X}$ and θ are represented as functions of (x, z). Consideration will only be given here to translation along the ridge, where $\bar{X} = \bar{X}[x, z(x)]$ and Θ = constant. The translation speed $c = c(x)$ of disturbances propagating over ridges of the same slope—but three different heights—is displayed in Fig. 4.

The variable translation is determined by the distribution of $\bar{u}_a[x, z(x)]$ on the ridge. This distribution is provided by BG (Fig. 4). There is a small region near the base of the ridge where $\bar{u}_a$ is negative and relatively weak. A relatively large positive gradient exists along the windward slope, and $\bar{u}_a$ reaches a maximum value ($\bar{u}_a|_{\max} > 0$) at the crest. In addition, $\bar{u}_a|_{\max}$ increases with the ridge height. The situation is reversed going downslope into the lee. These same features are exhibited in the translation speeds c shown by the curves in Fig. 4.

A relatively simple expression for c may be derived for a limiting case: the case of flow over a ridge produced by a doublet in an infinite atmosphere. In this case, the relationship

$$\bar{X} = \frac{xz}{2z - \Theta_0} \tag{23}$$

may be derived from BG (their Eqs. 33a, b) by letting $H \to \infty$ and by representing the lower boundary as $\Psi_0 \equiv \Theta_0$. The translation speed $c = dx/dt$ may be determined by requiring the phase $\bar{\chi}$, in either (21) or (22), to satisfy

$$\frac{d\bar{\chi}}{dt} = \left(\frac{\partial\bar{\chi}}{\partial x} + \frac{\partial\bar{\chi}}{\partial z}\frac{\partial z}{\partial x}\right)\frac{dx}{dt} + \frac{\partial\bar{\chi}}{\partial t} = 0. \tag{24}$$

Substitution of (23) into (24) yields

$$c = \frac{(2z - \Theta_0)^2}{2z^2 - (xdz/dx + z)\Theta_0}. \tag{25}$$

As in BG, the lower boundary may be expressed as $z = \Theta_0 + (\epsilon/D)h(x)$, where ϵ is the crest height, h represents the shape of the ridge and D is the deformation depth, $D = fL/N$. In this case of an infinite atmosphere, the only relevant parameter is ϵ/D, since the Rossby number Ro may be absorbed into the definition of the pressure or the geopotential. The translation speed is shown as a function of ϵ/D in Fig. 5. The increase in speed with ϵ/D is associated with the increases in $\bar{u}_a$ that accompanies either an increase in the crest height ϵ, in the slope ϵ/L or in the static stability N. This dependence, which has been discussed by BG (section 5), reflects conservation of the mass flux over the ridge. As a consequence, these parameters also control the translation of disturbances over a ridge. The speeds are lower at the ridge crest in an infinite atmosphere (Fig. 5a) than in a finite one (Fig. 5b), because the smaller gap between the lid and the crest promotes a more intense ageostrophic circulation.

5. Orographic frontogenetical features

It is evident in Figs. 2 and 3 that the steady mountain circulation alters the gradients of both the potential

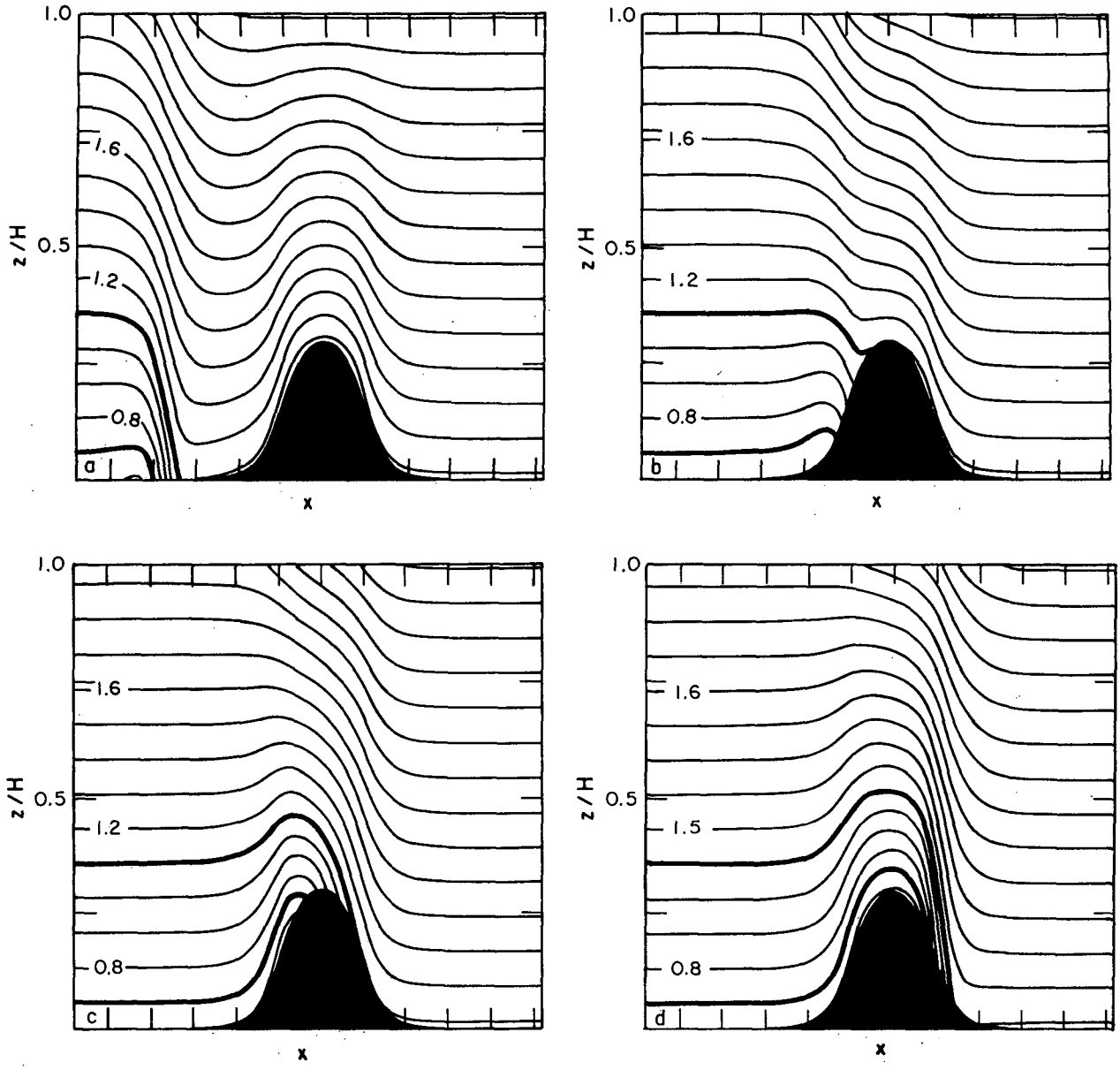

FIG. 2. Time sequence of the total potential temperature field $\Theta + \theta'$, defined by (15) and (21). The thick contours in each panel encompass the disturbance field delineated in Fig. 1a. (a) $T = 3$, disturbance upstream; (b) $T = 7$, center of the disturbance has ascended to the half-width of the ridge; (c) $T = 8$, disturbance situated at the crest; (d) $T = 9$, center of the disturbance has descended to the half-width of the ridge. A unit of time T corresponds to about 9.1 h.

temperature and the cross-stream velocity. The change in $\partial\theta'/\partial x$, for example, may be obtained from (11). The "frontogenetical" equation may be expressed as

$$\frac{d}{dt}\left(\frac{\partial\theta'}{\partial x}\right) = -\frac{\partial\bar{u}_a}{\partial x}\frac{\partial\theta'}{\partial x} - \frac{\partial\bar{w}}{\partial x}\frac{\partial\theta'}{\partial z}, \tag{26}$$

where d/dt represents the differential operator in (11). The first term on the right-hand side of (26) is the contribution to frontogenesis by horizontal *convergence*, and the second term represents the *tilting* of potential temperature surfaces by the vertical motion field. The contributions associated with each feature, in (26), and their sum appear in Figs. 6–8. The values are shown for the times that correspond to the relative positions in Figs. 2b–d.

Frontolysis is indicated on the windward slope (Fig. 6) in association with divergence of the ageostrophic velocity $\bar{u}_a$. This feature is antisymmetric, with the corresponding frontogenesis occurring on the lee slope. The gradient of vertical velocity satisfies $\partial\bar{w}/\partial x < 0$ in $-1 \leqslant x \leqslant 1$; otherwise $\partial\bar{w}/\partial x > 0$. Further, the leading

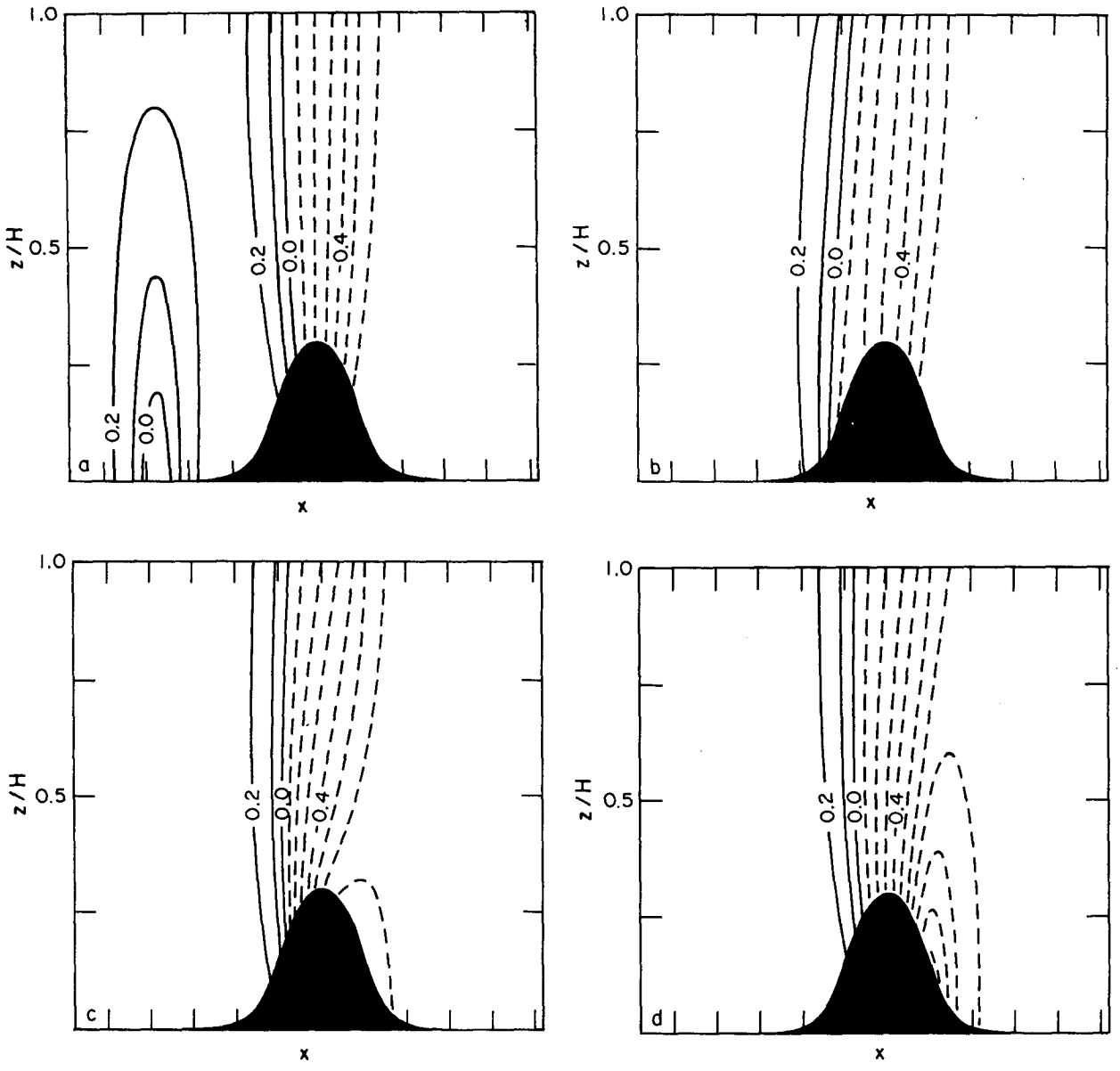

FIG. 3. As in Fig. 2, except for the total cross-stream velocity field $\bar{v}_g + v'$, where $\bar{v}_g$ denotes the steady solution and the disturbance v' is defined by (22). Dashed contours represent negative values.

edge of the θ' disturbance is characterized by $\partial\theta'/\partial z < 0$, as is evident in Fig. 1a. These features account for the particular antisymmetric pattern associated with the tilting terms, presented in Fig. 7, as the disturbance moves over the ridge. The total field, displayed in Fig. 8, is antisymmetric with equally broad regions of frontolysis and frontogenesis appearing on the respective slopes. The maximum value of frontogenesis (frontolysis) appearing on the slope is about a 0.13 K/100 km change in 3 h. This value is about an order of magnitude smaller than frontogenesis associated with an instability mechanism, (e.g., Blumen, 1980; Fig. 5). Frontogenesis in this latter situation is associated with rather intense time-dependent ageostrophic circulations, which have been omitted in this study.

Similar frontogenetical features appear when the cross-stream velocity is represented as a cyclonic shear zone by means of (21). Moreover, the largest value of frontogenesis (frontolysis) in the wind field, approximately 10^{-5} s^{-1} in a 3 h period, is about an order of magnitude smaller than the value obtained in the instability model presented by Blumen (1980; Fig. 7).

6. Ageostrophic circulation

The solutions presented in this study are exact solutions of the semigeostrophic system, (1)–(4), that sat-

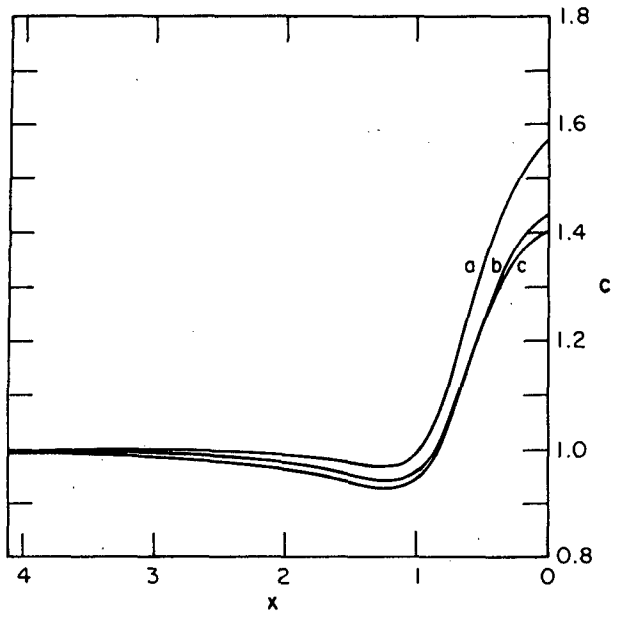

FIG. 4. Translation speed c along the ridge as a function of distance x, expressed in half-widths, measured either upstream or downstream from the crest situated at $x = 0$. The curves correspond to crests at the following heights: curve a, $\epsilon = 0.3H$; curve b, $\epsilon = 0.15H$; curve c, $\epsilon = 0.075H$. Note that c is scaled by the upstream current u_g.

isfy the boundary conditions (7) and (8). The absence of a constraint on the maintenance of thermal wind balance in the time-dependent disturbance field is a direct result of setting $u'_a = w' = 0$ in (9). Any imbalance, that occurs at time $t > 0$, is produced by translation through the steady mountain circulations ($\bar{u}_a$, $\bar{w}$). However, the following question may be raised: If thermal wind balance is disrupted at a particular instant of time, what are the characteristics of the circulation that would restore the balance? An answer to this question may be obtained by using (10) and (11) to provide the nondimensional expression

$$\frac{d}{dt}\left(\frac{\partial v'}{\partial z}-\frac{\partial \theta'}{\partial x}\right)=2Q, \tag{27}$$

where

$$2Q=-\left[\frac{\partial \bar{u}_a}{\partial z}\frac{\partial v'}{\partial x}+\frac{\partial \bar{w}}{\partial z}\frac{\partial v'}{\partial z}-\frac{\partial \bar{u}_a}{\partial x}\frac{\partial \theta'}{\partial x}-\frac{\partial \bar{w}}{\partial x}\frac{\partial \theta'}{\partial z}\right]. \tag{28}$$

Since (v', Θ') and their derivatives are conserved in (X, Θ, T) space, changes in the thermal wind balance expressed by (27) are brought about by both the tilting of the Θ surfaces and by the horizontal stretching associated with the geostrophic coordinate transformation (12). These are the same features that characterize frontogenesis in this model, and are discussed in section 5.

In principle, thermal wind balance may be maintained by an ageostrophic circulation determined by

$$\frac{\partial w}{\partial x}-\frac{\partial u'_a}{\partial z}=-2Q \tag{29}$$

as shown, for example, by Hoskins (1982). An evaluation of Q is presented in Fig. 9 at $T = 7$, when the center of the disturbance is situated at the half-width

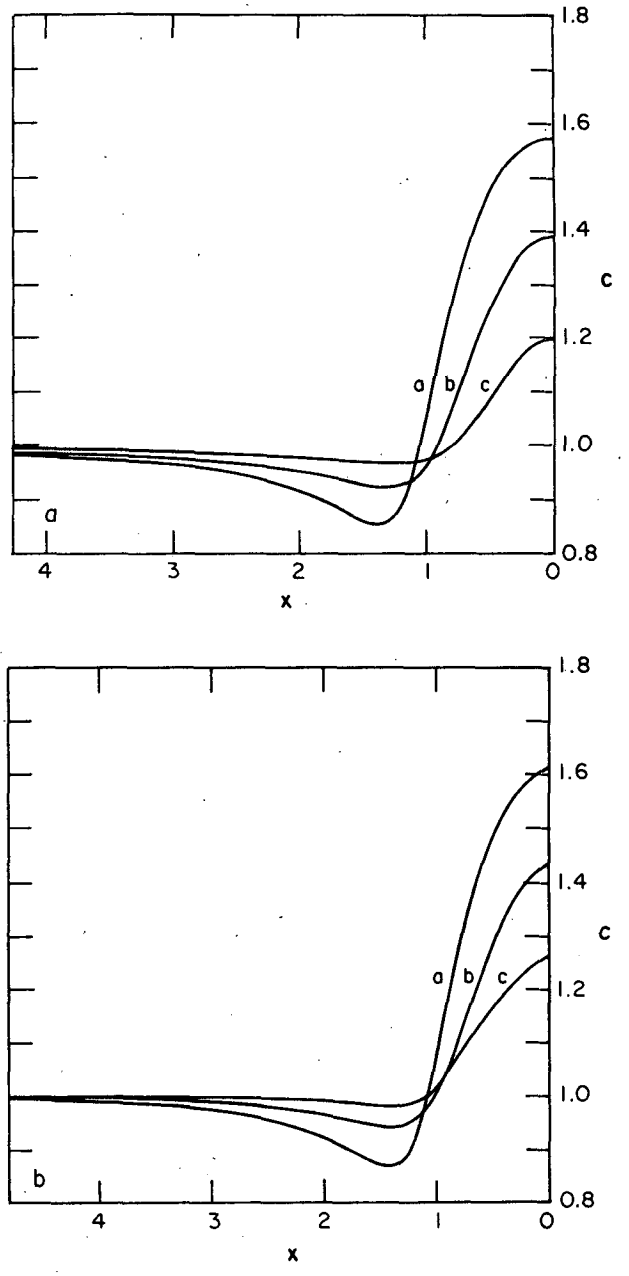

FIG. 5. Translation speed c along a ridge. Distance is expressed as in Fig. 4. (a) c in an infinite atmosphere ($H \to \infty$), expressed by (25). (b) c in a finite atmosphere for a disturbance moving over a ridge of height $\epsilon = 0.15H$. This value of ϵ provides the closest agreement with the values in (a). The variation of c is similar for other ridge heights ϵ, but differs in magnitude. The curves in each panel correspond to the following: curve a, $\epsilon = 0.6D$; curve b, $\epsilon = 0.4D$; curve c, $\epsilon = 0.2D$. Note that $D = fL/N$ is the deformation depth.

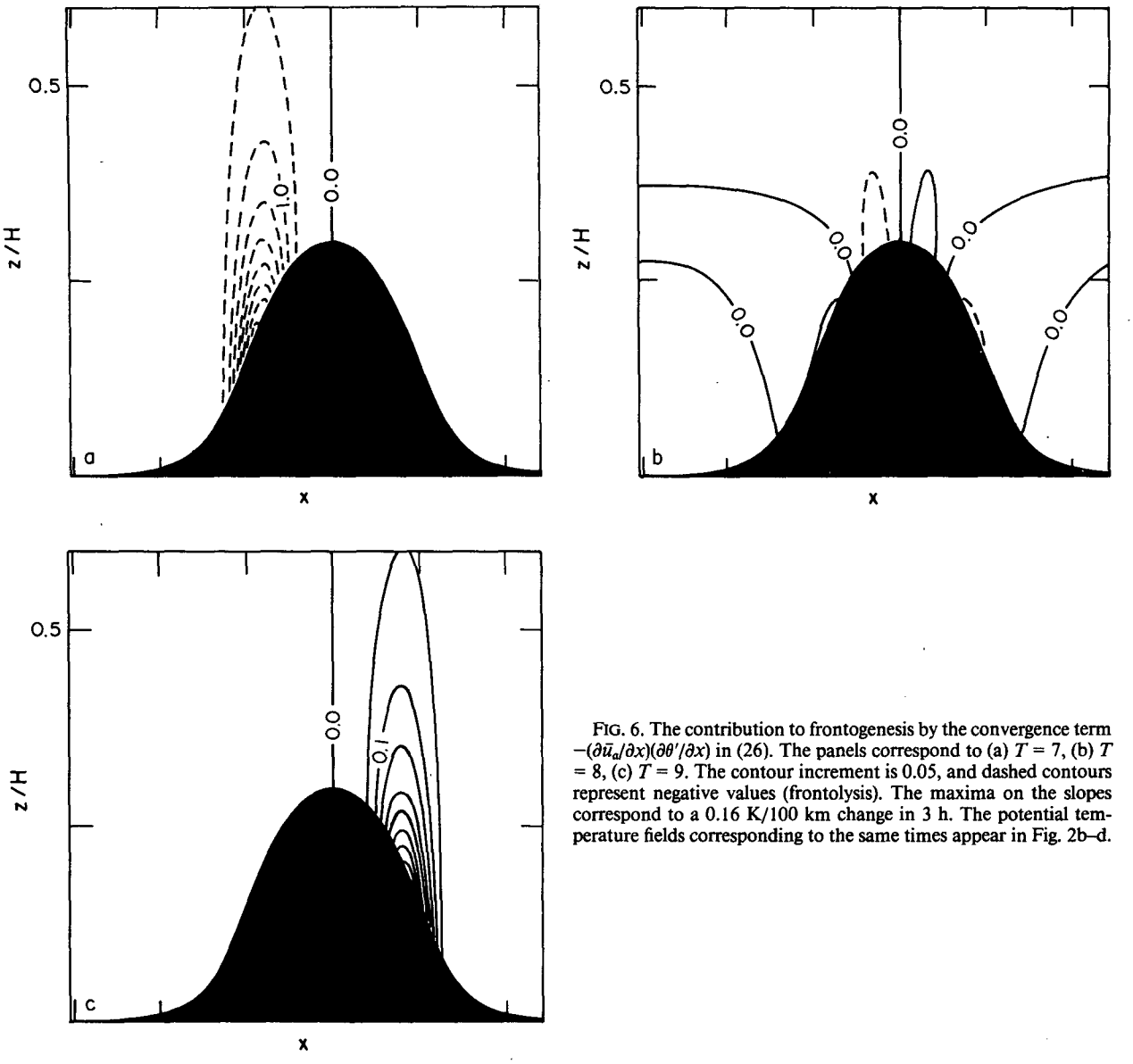

FIG. 6. The contribution to frontogenesis by the convergence term $-(\partial \bar{u}_a/\partial x)(\partial \theta'/\partial x)$ in (26). The panels correspond to (a) $T = 7$, (b) $T = 8$, (c) $T = 9$. The contour increment is 0.05, and dashed contours represent negative values (frontolysis). The maxima on the slopes correspond to a 0.16 K/100 km change in 3 h. The potential temperature fields corresponding to the same times appear in Fig. 2b–d.

of the ridge. Since $Q > 0$, the circulation required to restore thermal wind balance is an indirect circulation: clockwise around a horizontal axis. The situation is reversed on the windward slope. The dimensional values of Q, associated with the pattern of Fig. 9, are characterized by $Q \leqslant 2.5 \times 10^{-12}$ s^{-3}.

The dimensional expression for Q associated with the maintenance of thermal wind balance in the semi-geostrophic Eady instability model is characterized by

$$Q \approx -f^2 \frac{\partial u_g}{\partial z} \frac{\delta}{1+\delta}, \tag{30}$$

where $\delta = f^{-1}\partial v_g/\partial x$ is the ratio of the relative vorticity to the Coriolis parameter, and the constant shear of the basic flow is $\partial u_g/\partial z > 0$. In this case, a direct circulation ($Q < 0$) is required to maintain thermal wind balance. Values associated with intense surface frontogenesis (Blumen, 1980; Fig. 2) are $\delta \leqslant 4f$ with $\partial u_g/\partial z = 2 \times 10^{-3}$ s^{-1}. The values of Q are characterized by $Q \leqslant 1.5 \times 10^{-11}$ s^{-3}, which are about an order of magnitude larger than the values of Q associated with the pattern displayed in Fig. 9. This result is in accord with the specification of a relative weak upstream disturbance field, and the concomitant thermal wind imbalance established by the translation of this disturbance over the ridge.

7. Concluding remarks

Passive scalar disturbances are advected over a finite-amplitude ridge in a stratified, rotating atmosphere that

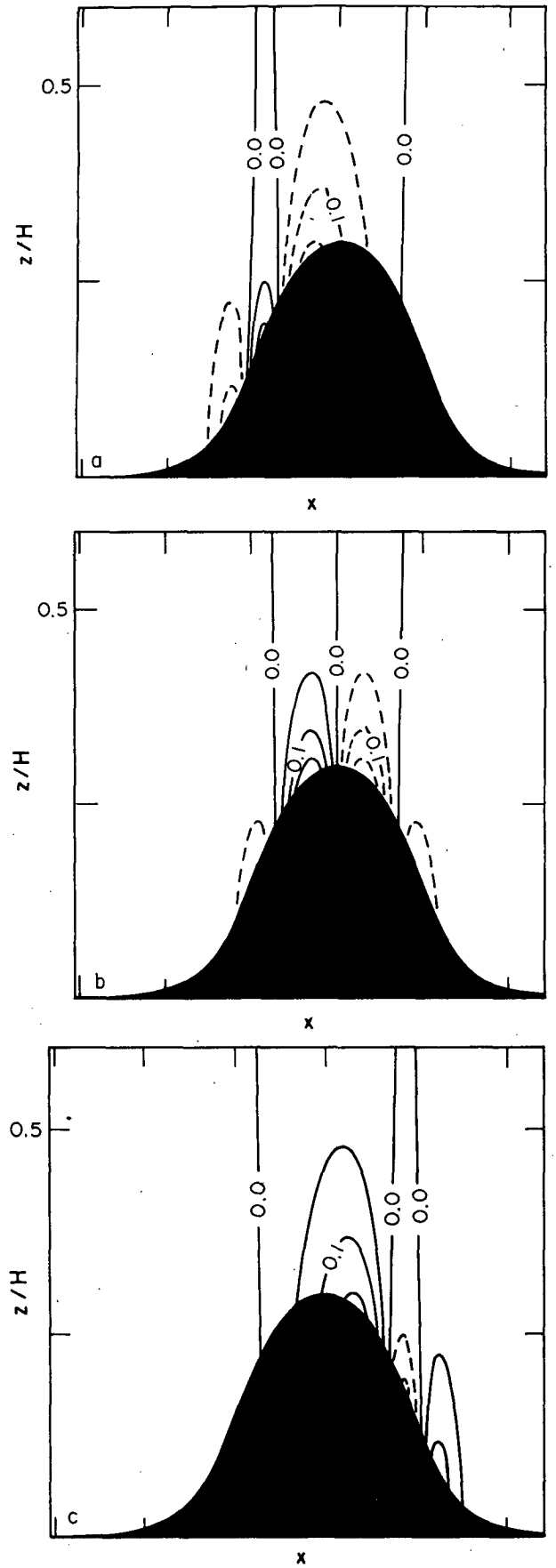

FIG. 7. As in Fig. 6, except tilting term $-(\partial\bar{w}/\partial x)(\partial\theta'/\partial z)$ in (26). The maxima near the ridge crest correspond to a 0.06 K/100 km change in 3 h in panels (a) and (c); the maxima in panel (b) correspond to a 0.07 K/100 km change in 3 h.

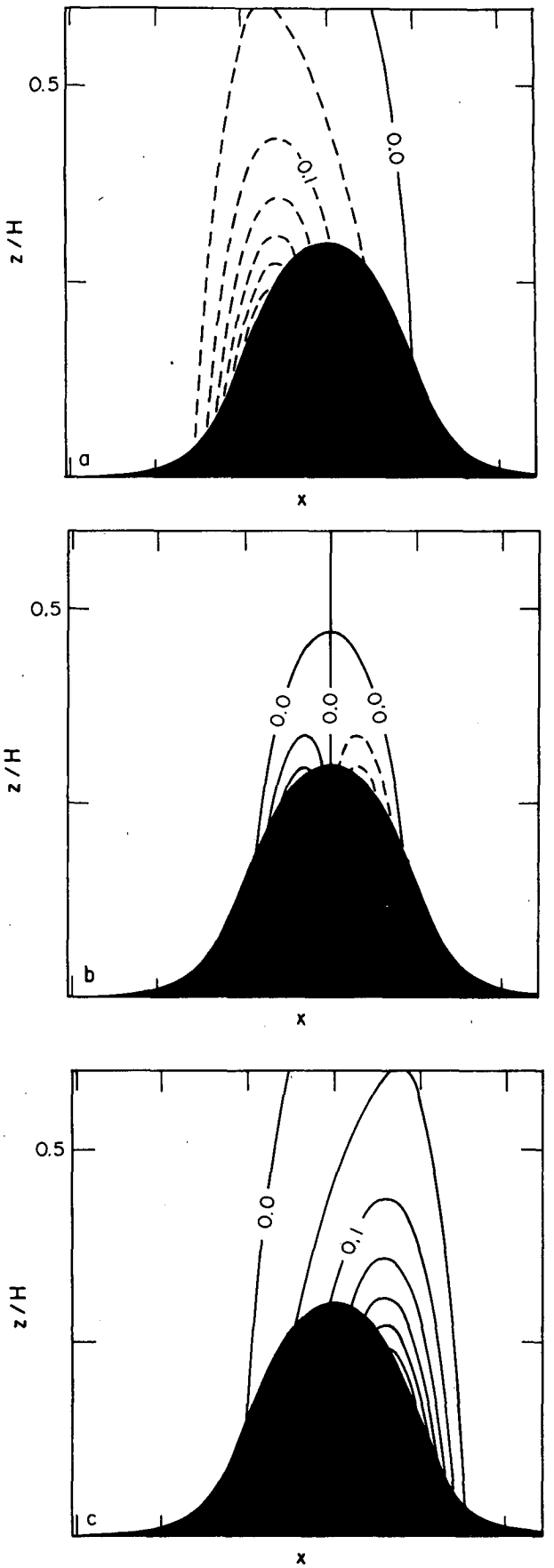

FIG. 8. As in Fig. 6, except sum of the convergence and tilting terms in (26). The maximum frontogenesis (frontolysis) $d(\partial\theta'/\partial x)/dt$ on the slopes corresponds to a 0.13 K/100 km change in 3 h.

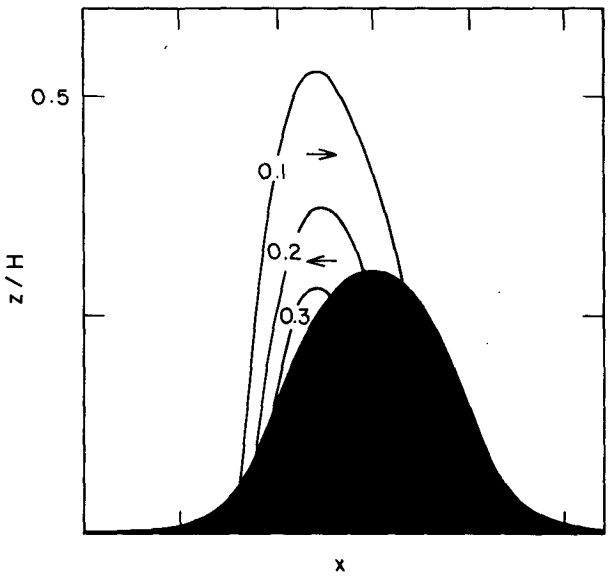

FIG. 9. Distribution of $2Q$, defined by (27) and (28), at $T = 7$ when the center of the disturbance has reached the half-width of the ridge. The term $2Q = 0.1$ corresponds to a dimensional value $Q = 0.075 \times 10^{-12}$ s^{-3}. The arrows denote the sense of the circulation required to restore thermal wind balance.

is capped by a rigid lid. The advecting velocity field is provided by a steady solution, representing the response to uniform flow over the same ridge. Since this steady mountain flow attains its maximum speed over the crest of the ridge, the disturbances are accelerated up the windward slope and decelerated on the downward leeward slope. This same feature of the mountain flow promotes frontolysis on the windward slope and frontogenesis on the leeward slope.

These features are not in agreement with Bannon's (1984) results because the derived mountain flow is different in each model. Bannon's mountain solution is characterized by downslope ageostrophic flow on both the windward and leeward sides of the ridge. The maximum divergence of this mountain flow occurs at the ridge crest, with smaller values of convergence near the base of the ridge. His conclusions regarding upslope retardation of the front and downslope acceleration in the lee, with frontolysis at the ridge crest, are in agreement with the properties of his mountain circulation. Nonetheless, the type of mountain circulation used by Bannon differs from the characteristic semigeostrophic solutions obtained by BG, Pierrehumbert (1985) and others. These latter solutions share the common property of a maximum ageostrophic velocity at the crest with the corresponding horizontal divergence field exhibiting the characteristics, discussed previously.

Results obtained from the present model are based on an exact solution of the semigeostrophic system of equations that satisfy a finite amplitude boundary condition. The solution represents the limiting case of a vanishing ageostrophic circulation associated with the disturbance field. Although application to the atmosphere is limited, the present results should be applicable to the propagation of weak disturbances over a ridge. The more complex problem of frontal interaction with orography may require the inclusion of an instability process that forces an ageostrophic circulation. The analysis would necessarily involve an evaluation of the mutual interaction between the circulations associated with both the mountain and the disturbance.

Acknowledgments. Financial support for this investigation is provided by the National Science Foundation under NSF Grants ATM-8313674 and ATM-8418625. The computations were carried out on the Pyramid 90X super minicomputer at the University of Colorado, Center for Atmospheric Theory and Analysis.

REFERENCES

Bannon, P. R., 1983: Quasi-geostrophic frontogenesis over topography. *J. Atmos. Sci.*, **40**, 2266–2277.

——, 1984: A semigeostrophic model of frontogenesis over topography. *Beitr. Phys. Atmos.*, **57**, 393–408.

——, 1986: Deep and shallow quasi-geostrophic flow over mountains. *Tellus*, 162–169.

Blumen, W., 1980: A comparison between the Hoskins-Bretherton model of frontogenesis and the analysis of an intense surface frontal zone. *J. Atmos. Sci.*, **37**, 64–77.

——, and B. D. Gross, 1986: Semigeostrophic disturbances in a stratified shear flow over a finite-amplitude ridge. *J. Atmos. Sci.*, **43**, 3077–3088.

Davies, H. C., 1984: On the orographic retardation of a cold front. *Beitr. Phys. Atmos.*, **57**, 409–418.

Hoskins, B. J., 1975: The geostrophic momentum approximation and the semigeostrophic equations. *J. Atmos. Sci.*, **32**, 233–42.

——, 1982: The mathematical theory of frontogenesis. *Ann. Rev. Fluid Mech.*, **14**, 131–151.

Huppert, H. E., and K. Bryan, 1976: Topographically generated eddies. *Deep-Sea Res.*, **23**, 655–679.

Kasahara, A. K., 1974: Various vertical coordinate systems used for numerical weather prediction. *Mon. Wea. Rev.*, **102**, 509–522.

Merkine, L. O., and E. Kálnay-Rivas, 1976: Rotating stratified flow over finite isolated topography. *J. Atmos. Sci.*, **33**, 908–922.

Pierrehumbert, R. T., 1985: Stratified semigeostrophic flow over two-dimensional topography in an unbounded atmosphere. *J. Atmos. Sci.*, **42**, 523–526.

——, and B. Wyman, 1985: Upstream effects of mesoscale mountains. *J. Atmos. Sci.*, **42**, 977–1003.

Robinson, A. R., 1960: On two-dimensional flow in a rotating stratified fluid. *J. Fluid Mech.*, **9**, 321–332.